Distribution and Fractionation of Uranium in Weapon Tested Range Soils

Joseph A. Kazery[1], Georgio Proctor[2], Steve L. Larson[3], John H. Ballard[3], Heather M. Knotek-Smith[3], Qinku Zhang[2], Ahmet Celik[2], Shaloam Dasari[1], Saiful M. Islam[2], Paul B. Tchounwou[1], Fengxiang X. Han[2,]*

[1] Department of Environmental Science, Jackson State University, 1400 J. R, Lynch St., Jackson, MS 39217

[2] Department of Chemistry and Biochemistry, Jackson State University, 1400 J. R, Lynch St., Jackson, MS 39217

[3] U.S. Army Engineer Research and Development Center, 3909 Halls Ferry Rd., Vicksburg, MS, 39180-6199

Abstract Uranium is a chemically toxic and radioactive heavy metal. Depleted uranium (DU) is the by-product of the uranium enrichment process, with a majority of U as uranium-238, and a lower content of the fissile isotope uranium-235 than natural uranium. Uranium-235 is mainly used in nuclear reactors and in the manufacture of nuclear weapons. Exposure is likely to have impact on humans or the ecosystem where military operations have used DU. Yuma Proving Ground in Arizona, USA has been using depleted uranium ballistics for 36 years. At a contaminated site in the Proving Grounds, soil samples were collected from flat, open field and lower elevated trenches that typically collect summer runoff. Spatial distribution and fractionation of uranium in the fields were analyzed with total acid digestion and selective sequential dissolution with eight operationally defined solid-phase fractions. In addition to uranium, other trace elements (As, Ba, Co, Cr, Cu, Hg, Mo, Nb, Pd, Pb, V, Zn, Zr) were also assessed. Results show that the trench area in the testing site had higher accumulation of total U (12.4%) compared to the open field soil with 279 mg/kg U. Among the eight solid phase components in the open field samples, U demonstrated stronger affinity for amorphous iron-oxide bound, followed by carbonate bound, and residual fractions, respectively. While U in the trench area had a stronger binding to the easily reducible oxide bound fraction, followed by carbonate bound, and amorphous iron-oxide bound fractions. Among other trace elements, Nb, As, and Zr exhibited the strongest correlations with U distribution among solid phase components. This study indicates a significant spatial variation of U distribution in the shooting range site. Fe/Mn oxides and carbonate were the major solid phase components for U in the weapon test site.

Keywords: Uranium, selective sequential dissolution, U fractionation, spatial distribution

INTRODUCTION

Uranium is a heavy metal that is chemically toxic and radioactive. Radionuclides of uranium in the Earth's crust dominate with uranium-238 as the most abundant isotope. Uranium is found in rocks, soils, water where it has been eroded and transported by water and wind[1,2]. The uranium-238 isotope is also the parent species in a long radioactive decay chain containing 16 radioactive elements[3].

Natural uranium consists of three isotopes: ^{238}U (99.27%), ^{235}U (0.72%), and ^{234}U (0.0054%). The concentration of ^{235}U is called "enrichment" that is used for nuclear energy and nuclear weapons[1,4]. With the half-life of 4.5 billion years, the radiation levels do not decrease significantly over time. However, almost half of the radiation is due to the ^{234}U isotope that is much more reactive than the other forms[2].

After the enrichment process, the uranium depleted of ^{235}U is called depleted uranium (DU) but DU may also be from reprocessing spent nuclear reactor fuel. Depleted uranium typically contains 99.8% ^{238}U, 0.2% ^{235}U, and 0.0006% ^{234}U by mass. These reduced proportions of uranium-235 and 234 account for about 60% the radioactivity released by natural uranium. There are minor applications for DU ranging from counterweights or ballasts in aircrafts. Due to its density twice that of lead, DU has been used for radiation shields in medical equipment and radioactive material containers. Military applications include armor-plate penetrating munitions, called penetrators, and reinforcing military vehicles[5,6].

Uranium poses multiple health risks. DU is a low radioactive α-emitter, therefore acute risk is not likely from external exposure. However, the potential hazard is a result from internal exposure. Due to its heavy metal nature, DU is also a chemical toxicant where the effects may be synergistic, therefore cannot be assumed to exclusively radiological or chemical effects[7]. Some

studies have observed that uranium from embedded DU fragments may redistribute in other systems, resulting in high levels of oncogenes that are associated with carcinogenesis.

Exposure is only likely to have a human or ecological impact where military operations have used DU. Exposure routes may involve dermal penetration of penetrators or armor due to shrapnel, or inhalation of DU dust upon impact. Also, ingestion is more likely for communities where large food supplies or drinking water becomes contaminated.[5,8,9] Ecosystem contamination occurs in the form of dust or stray shells on or in the ground[6].

There have been some studies that observe leachability of schoepite, DU corrosion, with the exchangeable fraction in sand-rich soils suggesting that 92% of dissolved U was held in other fractions in soil[10]. However, there are several other solid-phase fractions that are analyzed by selective sequential dissolution (SSD) that may dictate the transport of U. SSD has been used to investigate contaminated areas due to uranium harvesting, refining, etc.[11] While other studies have used artificially contaminated or spiked soils to better understand fractionation transport.[12,13] But little information is found on soil fractionations due to military use of DU and the long-term aging in soils (~38 years). One study of DU transport in Yuma, Arizona was conducted through analyzing various ecological levels, e.g. surface sediment (2-3 cm), vegetation, herbivores, and predators[14]. However, no analysis of soil U fractionation or soil burden of DU in active weapon testing ranges was documented.

The Yuma Proving Ground (YPG) in Arizona is a United States Army testing site that tests an array of projectiles and other ballistics. In specific areas, YPG deploys DU munitions, and has been testing DU since it was licensed by the Nuclear Regulatory Commission in 1982[14]. With a continuation of use, there has been little to no update on the status of DU at YPG in the last two decades. The objectives of this study are to evaluate the U contamination at YPG, to

spatially determine hotspots by analyzing soils located in the open field and the drainage trenches where summer runoff occurs at the gun position 20 (GP 20) site in YPG, to evaluate the fractionation of DU among solid phase components through SSD, to determine variations in U-bound soil fractions, and to determine the concentrations of other heavy metal or metalloids in the testing site.

MATERIALS AND METHODS

Study site and sampling

YPG is located near the Arizona-California border in the Lower Colorado River Valley of the Sonoran Desert. Based on climate data from 1961-1990, Yuma is extremely arid with a low average annual precipitation of 3.09 inches (78 mm), and average temperatures reaching a high of 107°F during summer and a low of 46°F during winter[15]. However, rainfall is sporadic and high intensity flash floods cause erosion and significant runoff[14]. The valley is composed mostly of sand and sedimentary deposits as rivers have cut through the mesa when the valley was forming. Yuma has been recognized to have six types of soil: imperial sand, imperial sandy loam, imperial fine sandy loam, imperial silt loam, imperial loam, and Salt River Adobe[16], However, the valley at YPG is a stony alluvial fan being described as a gravelly sandy loam. The sandy components allow for good drainage in the soil, with water passing through rapidly[17].

Gun Position 17 (GP 17) and Gun Position 20 (GP 20) are two areas at YPG that test DU penetrators. During June of 2018, twenty locations were randomly sampled in the open field area of GP 20 to a depth of 15 cm, along with 10 other locations at the drainage trenches where runoff is drained and is transported (Fig. 1). The entire sampling area was determined to be 2,965 m^3.

Chemical analyses

All samples were processed in triplicate with reagent blanks for quality assurance/quality control. Due to background soils containing significant amounts of TEs, the real soil would not be ideal for determining the detection limits as defined as blank[18]. All glassware and Teflon tubes used were washed with HNO_3 and rinsed with deionized water.

Soil characterization

Fifty-milliliter polypropylene digestion tubes were used during soil characterization experiments. The pH was measured in 1:1 soil-water saturated paste with an Oakton p110 series pH meter, that was calibrated at pH 4, 7, and 10.[19] Electrical conductivity was also measured in the same saturated paste with a Fisher brand Traceable conductivity meter[20]. The pH and conductivity were only processed as one per location. Organic matter (OM) was determined with the $K_2Cr_2O_7$-H_2SO_4 method and carbonate was determined with the gravimetric method for loss of carbon dioxide[21]. Texture of particle size was determined by the hydrometer method using an ASTM 152H Soil Hydrometer standardized at 68°F[22,23]. Active iron- and manganese-oxides were analyzed with the citrate-bicarbonate-dithionite method[21].

Total concentrations of U and other trace elements

The total concentrations of uranium and other trace elements (As, Ba, Co, Cr, Cu, Hg, Mo, Nb, Pd, Pb, U, V, Zn, Zr) were determined with 4 M HNO_3 soil extraction for 20 soils from the field and 10 trench samples in triplicates. This extracted trace elements (TEs) bound in the soil matrix. Twenty-five mL of 4 M HNO_3 was added to 1 g of fresh soil in a 50-mL polypropylene digestion tube. Extraction was carried out in an 80 °C water bath for 16 hours[24,25].

Samples were diluted and analyzed with a Varian 820MS inductively coupled plasma- mass spectrometer (ICP-MS), Australia.

Characterization of Uranium

X-ray powder diffraction (XRD) (MiniFlex 600, Rigaku, Japan) was used to analyze soil samples. Oxidized uranium from the trench was analyzed at one location in replicate. XRD analysis was performed with an accelerated voltage of 45kV and a current of 15mA. Data was recorded in the 10-80° range with a step of 0.02° and a 5°/min speed. Results were compared against standards, UO_3 (JCPDS# 15-0201), and JADE software. A Ludlum model 703e was used to determine radioactive isotope present.

Selective Sequential Dissolution (SSD) Procedures

Fractionation of U and other TEs were analyzed in eight operationally defined solid-phase fractions with SSD. This determination was based on the procedure developed by Tessier et al.[26], Han and Banin[27], and Han el al.[25]. This procedure extends further with the addition of a water-soluble fraction as used by Aigberua[28].

Water-soluble trace elements (SOL)

This soluble fraction consists of TEs that are weakly bound in soils and are readily bioavailable to the environment[27,28]. Water-soluble TEs were extracted with 25 mL of distilled water at pH 7.0 added to 1 g of fresh soil in a 50-mL Teflon centrifuge tube. The mixture was shaken for 2 h at 28°C. The mixture was then centrifuged at 6000 rpm for 10 min. The supernatant was decanted and filtered through a 0.45-µm filter. Due to the high concentration of

DU the filtrate was further diluted 50X in 5%HNO_3 for ICP-MS analysis. The soil residue was kept for the next fractionation. The same centrifugation, decantation, and dilution steps were used for each subsequent extraction.

Exchangeable trace elements (EXC)

The exchangeable fraction is extracted with ionic composition exchanges in water that affect sorption of TEs to major soil constituents[26]. The soil residue from the SOL fractionation was extracted with 25 mL of 1 M NH_4NO_3 solution that was adjusted to a pH of 7.0 with NH_4OH. The mixture was shaken for 30 min at 28°C. Due to retention of solution when decanting centrifuged supernatant, all proceeding fractions after the SOL fraction were calculated using the following equation:

$$\mu_g \text{ extracted} = C \times 25g - C' \times M$$

where C is the concentration (μ_g/g) of TE in the current fraction extracted, C' is the concentration (µg/g) of TE in the previous fraction extracted, and M is the mass (g) of solution carried over from the previous extraction to the current extraction[24].

Carbonate bound trace elements (CARB)

The carbonate fraction consists of TEs bound to carbonates in soil. This fraction is affected by changes in pH[26]. The soil residue from the EXC fractionation was extracted with 25 mL of 1 M CH_3COONa-CH_3COOH buffer solution at pH 5. The mixture was shaken for 6 h.

Trace elements bound to easily reducible oxides (ERO)

The easily reducible oxide fraction consists of TEs bound to Mn oxides that are easily reducible in anoxic conditions[25]. The soil residue from the CARB fractionation was extracted with 25 mL of 0.1 M $NH_2OH \cdot HCl$+0.01 M HCl at pH 2 and shaken for 30 min.

Organic matter bound trace elements (OM)

The organic matter fraction consists of TEs bound microorganisms as well as other soil organics. When oxidized organic matter can release TEs[25,26]. The soil residue from the ERO fractionation was mixed with 3 mL of 0.01 M HNO_3 and 5 mL of 30% H_2O_2 and digested in an 80°C water bath for 2 h. Additional 2 mL of H_2O_2 were added and was heated for 1 h. Then 15 mL of 1 M NH_4NO_3 was added and shaken for 10 min.

Trace elements bound to amorphous iron oxides (AmoFe)

This fraction consists of TEs bound to amorphous iron oxides. The residue from the OM fractionation was extracted with 25 mL of 0.2 M $(NH_4)_2C_2O_4$-0.2 M $H_2C_2O_4$ at pH 3.25 and shaken in the dark for 4 h.

Trace elements bound to crystalline iron oxides (CryFe)

This fraction consists of TEs bound to crystalline iron oxides. The soil residue from the AmoFe fractionation was mixed with 25 mL of 0.04 M $NH_2OH \cdot HCl$ in 25% acetic acid and digested in 97-100°C water bath for 3 h.

Residual trace elements (RES)

The residual fraction contains TEs that are not released into a solution from all previous steps. These TEs are found in crystalline structures of primary and secondary minerals, as well as from incomplete extractions from the previous fractions and organic matter such as humic acid[25,26,28]. The extraction procedure for residual TEs is the same for the total trace element procedure. The soil residue from the CryFe fractionation was mixed with 4 M HNO_3 and extracted in an 80°C water bath for 16 h.

Data analysis

Soil concentrations of U and TEs in different areas or fractions were analyzed with analysis of variance single factor (ANOVA) and regressions using Microsoft Office Excel to determine significance or correlations. Significant differences were considered for p values less or equal to 0.05. Area characterization and image analysis were done using ArcGIS 10.6.

RESULTS AND DISCUSSION

Soil characterization and properties

The soil surface of the general field was characterized as being a desert torched pavement, very arid and of sparse vegetation[14,17]. The subsoil was characterized by a majority of sand (51.83%) and silt (32.08%) and low amounts of clay (16.09%) (Table 1). As seen in Table 1, the soils collected in the field at GP20 at YPG were basic averaging a pH of 8.21. Compared to the trench the differences were significant ($p<0.05$), ranging from slightly acidic to basic with a pH of 6.79 to 8.31. Electrical conductivity is a measure of soluble salt content in saturated soils[20], these ranged greatly in all samples. This is described where salt content has been found to be magnitudes higher than nearby soils depending if gravel pavements are present[17]. Calcium

carbonate ranged from 8.33 to 34.15% (Table 1). However, these values were ten times higher than those reported by Holmes et al.[16]. The higher percentage of calcium carbonate was expected since desert soils contain a prominent calcic horizon that is shallow and typical of arid regions[29]. Organic matter was relatively high averaging a value of 3.06% that has been observed by others[16] and may be due to microbial activity[17].

U minerals in soil of Yuma site

Using the isotope identifier, Uranium-238 was the dominant radioactive isotope observed in the samples. Bright yellow oxidized uranium from penetrators was abundant in trench soils. Upon analysis by XRD of the corroded products, schoepites were present as the major mineral family at both locations. Their XRD patterns resemble that of uranium (VI) oxide hydrate ($UO_3 \cdot 2H_2O$) (Fig. 2). Under field conditions, this has been observed to be the dominant corrosion product of U in sand[10]. Uranium of this oxidation state is also referred to as uranyl species. Compared to the UO_2 species, UO_3 and uranyl are more soluble and likely to be found in surface water[30,31]. This may explain the appearance of schoepite minerals found in the top surface of the deep buried penetrators in the field through the upward movement of U as uranyl form and redeposited at the surface. This upward movement may be caused by solubility of U in schoepites in soil pore water and was transported driven by high evaporation forces in desert landscape[32]. Moreover, corroded products of penetrators from the open field contain silicates in soils.

Spatial distribution of uranium in fields

The total content of uranium found in the general field of GP 20 along with the trench is reported in Table 2. Using ArcGIS, the areas of each sample location were determined. Using the area of the trench, 338 m^2, and the total area of 2,965 m^2, the weighted average of the sample area was 14,430 mg/kg U.

Analyzed separately, the trench U was significantly higher, being 2.65 magnitudes higher than the open field samples, $p<0.0001$. Due to this statistical difference, the open field was considered sufficient when determining correlations. The uranium concentration from the trench samples ranged from 18,960 to 287,900 mg/kg, with a mean of 124,400 mg/kg. This mean was 446 times higher than the open field mean. The open field samples ranged from 13 to 2,282 mg/kg, averaging 278.8 mg/kg U.

Natural background levels of U in soils was 2 mg/kg[31], that is in a close agreement with other ranges (0.05 to 4.7 mg/kg) that have been reported in Qatar[33]. But due to a more local study of California soils, the U concentration was determined to be slightly higher ranging from 1.2 to 21.3 mg/kg, with the mean of 3.8 mg/kg[34]. Comparing the weighted average to the California concentrations, our sample site was approximately 3,800 times more contaminated than normal background levels.

Over two decades ago Ebinger et al. sampled YPG. Their sample plots were chosen nonrandomly, where penetrator impact sites were closely clustered together and transected areas of high biodiversity, such as trenches and wash areas[14]. Their sample site was 3,000 to 3,500 m down the firing line from the gun position at GP 20[14]. These impact sites can easily be observed as impact craters of displaced soil, as seen around our study site in Figure 1. The U concentration from the study by Ebinger et al. ranged from 0 to 1,400,000 mg/kg between 22 samples (Table 2). Our sampling area was approximately 4,000 to 4,060 m from the gun position down the firing

line. Samples from our study were 500 m further down the firing line. When comparing both trench samples even though the U maximum from the 1996 study was nearly 4.8 times as high, they found to be statistically similar. However, since total values were simple they may be a conservative method of quantifying contamination[35], a further breakdown of U among geochemical components was insightful.

U fractionation among solid phase components

Selective sequential dissolution (SSD) of U was conducted for both open field and trench soil locations to observe variation. SSD allows for one to determine the leachability of trace elements based on chemical reagents used. This allows to analyze the specific geochemical components[36], i.e. solid-phase fractions, in soil to follow the transport and bioavailability of U. Statistical summaries of both locations are presented in Table 3. All soil fractions extracted from the open field samples were shown to be significantly different from the fractions extracted from the trench soils. The fractions SOL, EXC, CARB, ERO, and AmoFe showed probability levels to be less than 0.001. Whereas the OM, CryFe, and RES fractions had probability levels less than 0.05. Uranium was mostly present in the AmoFe fraction followed by the CARB fractions of the open field soil. However, in the trench soil the ERO fraction was dominant, followed by the CARB and AmoFe fractions, respectively.

No U was found to be extracted in the water-soluble (SOL) fraction from the open field due to being well below the detection limit. The SOL fraction in the trench samples were found to have a mean of 421.1 mg/kg U. The SOL extraction being pure water is a solution that may be the most analogous to runoff or sediment pore water. Of the reagents used during extraction, this is most similar to the natural pH of soils in dry climates, as well as our sample site, Table 1. The

U concentration in trench's EXC fraction was 2,200 mg/kg, a 2.59 order of magnitude higher than the open field EXC fraction of 5.699 mg/kg. One can visually observe the percentage of variation of each fraction between sampling locations in Fig. 3. The SOL and EXC fractions both made up a small portion of U, being approximately 5% of the total at each location. These results are much lower than those reported in wetland environments that have been shown to contain 31% U in their SOL and EXC fractions which are attributed to a higher level of organics[37]. However, our results are in agreement with other studies of similar locations and indicate that the leachability of U from Yuma ranges was significant since soluble and exchangeable forms are the most mobile and bioavailable[36] being on the surfaces of clays, minerals, and organic matter[25]. It has also been demonstrated that U was not correlated with clay and that it did not bind to clays by cation exchange[37].

The trench's mean CARB fraction contained 27,860 mg/kg U. This was 2.77 orders of magnitude higher than the open field CARB fraction of 47.32 mg/kg U. In Fig. 3, the percentage of U in the CARB were similar, being 20% and 21% of the total U in the trench and field, respectively. This was less than that reported by Johnson et al.[38] on the CARB fraction of 55-94 % from DU from penetrators that had been exposed for 22 years. Possible decrease could be due to redistribution of U into a less labile fraction over time. The amount of U found in the CARB fraction may be attributed to the high amount of carbonate that is commonly found in arid soils. In soils with high amounts of carbonate, elements may have a low availability due to the precipitation with carbonate[39]. Also, sorbed elements may be occluded in pore spaces[37,40]. This greatly decreased the availability of U. Being less available and more stable is due to elements diffusing deeper in a solid-phase structure[37].

The CARB extraction has a pH most similar to that of rainwater which has the ability to cause temporary acidification or leaching during flash floods. However, carbonate dissolution does not occur at near neutral states above pH 6, [41] and due to similar alkaline soil pH in the open field area this may not be likely unless pH or reduction potential changes[42,43].

With exception of the SOL fraction, the lowest U mean concentration from the open field fractions was ERO 0.0813 mg/kg, whereas the trench samples presented the highest concentration of 94,020 mg/kg, Table 3. This was the largest variation being 4.28 orders of magnitude higher in the trench samples. This variation could also be observed in Figure 3. The U distribution in the ERO of the open field was far less, 0.04%, than the fraction in the trench, 68.90%. The low U field concentration bound to easily reducible oxides may also be related to potential transformation into other fractions during periods of reduction process[44].

The ERO are well associated with manganese oxides[27,45,46] and there is typically an increased amount of manganese in areas of runoff[47]. The transfer of the easily reducible oxides in trenches suggest a mild acidic or reductive shift of manganese oxides that U is bound with during storm events. This is supported by easily reducible oxides occurring with acidic soils[47] and some of the trench samples being slightly acidic (not shown).

The OM fraction also was represented by a low concentration of U from the open field and the trench, 0.5621 and 18.04 mg/kg respectively (Table 3), as well as a low proportion of the total fractions, 0.25 % from the open field and 0.01 % from the trench (Figure 3). The OM fraction was closely associated with U bound to readily oxidizable organic matter[37,46]. Organic matter is very low, which is typical of this environment (Table 1).

The AmoFe fraction from the open field showed the highest concentration of U averaging 139.4 mg/kg (Table 3), making up 63.13% of the total fractions (Figure 3). The trench samples

showed U bound to AmoFe as the third highest concentration of 11,750 mg/kg, making up 8.61% of total fractions from the trench. When observing this fraction and the other iron-oxide fraction (CryFe) there was a noticeable decline in U in the crystalline iron-oxides. The U proportion in the CryFe was only 1.01% of the open field fractions and even less in the trench at 0.10%. This has been documented in other studies indicating that U adsorbs to amorphous iron-oxides more strongly than crystalline iron-oxides, having a greater surface area[48,49].

Having a lower concentration in the crystalline iron-oxides may further demonstrate the lack of time or redox effects in this arid area that would further incorporate U into the more stable crystalline iron-oxides. This is observed by previous studies where TEs in amorphous iron-oxides thermodynamically transform into the more stable crystalline iron-oxides with age[50,51]. However, this condition of less CryFe may also be due to sorption inhibiting crystallization[52] and potentially high solubility and leachability of schoepites in soils.

The residual U left after the SSD procedure was determined by the RES step. This was generally a low amount, extracting 25.56 and 65.74 mg/kg from the open field and trench, respectively. However, the RES made up 11.57% of the open field with the trench representing 0.05% of U extracted at this fractionation. The open field U was similar with the results of a contaminated wetland where contaminated U was found to be 11 to 17% of the residual fraction[37]. Uranium most likely migrated to the RES by dissolution and adsorption over time to more stable, less labile silicate clays and amorphous silica.

Soils display high heterogeneity due to constant flux from biogeochemical processes or constant contamination from anthropogenic inputs[53]. Equilibrium does not commonly occur in soils. However, with ample time, and stable conditions, metals have been shown to redistribute into different solid-phase components, being considered nearer to an equilibrium. This may be

concluded if observing two fraction-distributions of similar patterns and was suggested by Han et al.[54] that as distribution patterns become more consistent with parent soils, metals were becoming more stable and were less likely to redistribute. From long-term field studies we could observe a more comparable distribution. In one such study, a 22-year period in an arid carbonate-rich environment demonstrated that the majority of U was bound to carbonate at various depths, followed by clay silicates and amorphous silica and the more labile soluble fraction in the lower depths of 15 cm[38]. This seemed to be in contrast to the current study where the majority of U was found with Fe/Mn-oxides, followed by carbonates, the residual fraction associated with silicates and amorphous silica, and the more labile soluble fraction. While the 22-year study was conducted at undisturbed penetrators, the present study reflected a more random collection of contaminated samples that have been accumulating DU for an additional 14 years. This may assume the current study has a more stable and realistic distribution.

Other correlations were determined for total U with other chemical properties. The field samples demonstrated a medium negative Pearson's correlation with manganese oxides ($R = -0.56$), organic matter ($R = -0.41$), and iron-oxides ($R = -0.39$), all significant. These negative relationships were not expected, where in wetland environments high in organic matter has been shown to hold a 37 to 57% of U[37]. These negative correlations in this study indicate that these chemical constituents may hinder total U concentrations. Similar results were observed by Bednar et al.[55] who demonstrated that organic matter actually hindered U sorption and may compete with binding sites on oxides or clays. It was also proposed that U molecules were too large and could not fit any organic matter structures and are out-competed by other trace elements[33]. The current data suggest that the total U concentration is largely controlled and can

be explained by the variability of manganese-oxides followed by organic matter, then iron-oxides as indicated by their R-square values that indicate that 31%, 17%, and 15% respectively.

Total concentrations of other trace elements

Total concentrations of all other TEs (As, Ba, Co, Cr, Cu, Hg, Mo, Nb, Pd, Pb, V, Zn, Zr) are reported in Table 4. In the open field samples, Ba had the highest concentration, 429.2 mg/kg, being more abundant than U with a mean of 278.8 mg/kg. This concentration of Ba was natural background, a national mean of 400 mg/kg across the United States[56]. In the trench the Ba concentration fell to a mean of 220.0 mg/kg. Most TEs decrease in concentration from open field to trench samples (Table 4). This was not true for U that demonstrated a 2.65 magnitude increase. Mercury also increased in the trench but was determined to be statistically similar. This increase may be due to the abundant input of U in solid colloidal or particulate form, and was easily transported by environmental factors such as rain or runoff, rather than thermodynamic factors in the soil.

Between both sample locations it was determined that all TEs, except for Hg and Mo, exhibited significant differences. This further reinforced the decision to only use the open field sample locations for correlation and not to combine the two. The decreasing order of TE and U concentrations in the open field was Ba > U > Zn > V > Cr > Cu > Pb > Zr > Co > As > Pd > Mo > Hg > Nb. In the trench, this order of decreasing concentrations was U > Ba >Zn > V > Cu > Cr > Zr > Pb > As > Co > Pd > Mo > Hg > Nb. The order of concentration at these sample locations, other than U and Ba, varied by Cu being more abundant than Cr and As being more abundant than Co in the trench samples.

Presence and variation of other trace elements among solid phase components in the field

Among all trace elements, U distribution among solid phase components was unique, heavily in the AmoFe fraction, followed by the CARB fraction. In comparison of the open field U to the other trace elements (As, Ba, Co, Cr, Cu, Hg, Mo, Nb, Pd, Pb, V, Zn, Zr), typically Ba was more present at the natural background level across the United States. In this study we determined Ba mean to be 429 mg/kg and was the most abundant TE observed in this study. Interestingly, while running SSD it was frequently observed that Ba seemed to have a negative correlation with U, $R = -0.24$, $p<0.001$. When ranking U amongst other trace elements from the higher U contained fractions, the AmoFe fraction U outcompeted all other analyzed elements with a concentration of 139.3 mg/kg. Having an order of decreasing concentrations as U > Ba > Zn > Cu > Zr > V > Cr > As > Pb >Nb > Co > Mo > Pd > Hg (Table 5). In the CARB fraction, U had the second highest concentration of 47.03 mg/kg, falling behind Ba with 85.6 mg/kg. The order of concentration in the CARB fraction was Ba > U > Cu > Cr > Zn > V > Mo > Hg > Pd > As > Nb > Co ~ Pb, the lowest two trace elements below the limit of detection (Table 5). The RES fraction, other than Ba, favored Zn over U, making up 26.73 mg/kg of this fraction. The order of concentration for the RES was Ba > Zn > U > V > Cr > Cu > Zr > Pb > Co > As > Pd > Hg > Mo > Nb. With exception of U, this fraction showed the most similar order to the total concentrations as seen in Table 5. This may imply, that regardless of the amount reclaimed at this fraction, these elements were more present in the clays and amorphous silica.

Even though a low percentage of U was found in the EXC fraction, it constituted one of the major elements, 5.70 mg/kg, in that fraction, Ba > U > Zn > Cr > V > Mo > Co > Cu > As ~ Zr ~ Nb ~ Pd ~ Hg ~ Pb. Samples found in the SOL, OM, ERO, and CryFe fractions showed

similar results as several other TEs such as Ba, V, Zn, Cu, and Cr consistently outcompeted U in these fractions.

Establishing element relationship among soil fractions may assist in determining if a viable alternative to U may occur. Pearson's correlations were calculated from the percentages of U and each of the analyzed TEs (As, Ba, Co, Cr, Cu, Hg, Mo, Nb, Pd, Pb, V, Zn, Zr). When observed across all eight fractions Nb, As, and Zr demonstrated a strong correlation with U; showing correlation coefficients (r) of 0.94, 0.93, 0.85, respectively. Pd, Cu, and Mo demonstrated a moderate correlation, with r values of 0.59, 0.48, 0.32, respectively, while other TEs such as V, Cr, Zn, Ba, Pb demonstrated a low correlation ($r < 0.30$), or low negative correlation as recorded for Co and Hg. Many of the correlations were not statistically significant. Being a field study, these correlations would only be practical in our present situation or environment, inferring that these results may not occur outside of these samples. Compared to U, Nb or Zr had a low toxicity and a strong U correlation. Both Nb and Zr were observed in high percentage, 98% and 59% respectively, in the AmoFe fraction, which corresponded with the highest U percentage at 63%. However, other TEs shared comparable percentages with U at various fractions, i.e. Ba (22%) and Cr (23%) with U (21%) at the CARB fraction, or Cr (1.6%) and Zn (3.5%) with U (2.6%) at the EXC fraction. This may be used to determine alternatives to U at fraction-specific conditions.

Conclusion

In Yuma Proving Ground at Gun Position 20, for almost four decades DU has been used and continually accumulating. When considering the sampled area, the total weighted average was determined to be 14,430 mg/kg. The high elevated open field was determined to contain 279 mg/kg U

while the low elevated trenches where drainage accumulates contained 124,416 mg/kg U. Compared to the trench concentrations collected 22 years early from another study, the present study was approximately half the earlier U concentrations.

Selective sequential dissolution allows insight for land management practices by determining leachability of U. About 3% of U was found in the labile EXC fraction in the high elevated open field and only 2% in the trench. Being carbonate-rich location, 20 - 21% U in open field and trench was found in the CARB fraction. The open field sequestered the majority of U, 63%, in amorphous iron which is a more-stable fraction. However, the majority, 69%, of U in the trench was determined to be in the easily reducible fraction that is more likely to become available during times of saturation. The most stable residual fraction sequestered 12% of the open field U, interestingly U found in the trench was 0.05%. However, the trench did contain 9% of its U in a more stable amorphous-iron fraction.

ACKNOWLEDGMENTS

This study was supported by the U.S. Army Engineer Research and Development Center (W912HZ-16-2-0021), the U.S. Nuclear Regulatory Commission (NRC-HQ-84-15-G-0042, NRC–HQ-12-G-38-0038, and NRC-HQ-84-16-G-0040) and the U.S. Department of Commerce (NOAA) (NA11SEC4810001-003499, NA16SEC4810009, NOAA Center for Coastal and Marine Ecosystems Grant # G634C22).

REFERENCES

(1) Asica, A.; Kurtovic-Kozarica, A.; Besica, L.; Mehinovicc, L.; Hasicc, A.; Kozarica, M.; Hukica, M.; Marjanovica, D. Chemical Toxicity and Radioactivity of Depleted Uranium: The Evidence from in Vivo and in Vitro Studies. *Environ. Res.* **2017**, *156* (December 2016), 665–673. https://doi.org/10.1016/j.envres.2017.04.032.

(2) Environmental Protection Agency (EPA). Radionuclide Basics: Uranium https://www.epa.gov/radiation/radionuclide-basics-uranium (accessed May 22, 2019).

(3) Salama, E.; El-kameesy, S. U.; Elrawi, R. Depleted Uranium Assessment and Natural Radioactivity Monitoring in North West of Iraq over a Decade since the Last Gulf War. *J. Environ. Radioact.* **2019**, *201* (January), 25–31. https://doi.org/10.1016/j.jenvrad.2019.01.017.

(4) URANIUM, ELEMENTAL http://toxnet.nlm.nih.gov/cgi-bin/sis/search2/r?dbs+hsdb:@term+@DOCNO+2553 (accessed May 22, 2019).

(5) World Health Organization. *Depleted Uranium : Sources , Exposure and Health Effects*; 2001.

(6) Parker, H. M. O.; Beaumont, J. S.; Joyce, M. J. Passive , Non-Intrusive Assay of Depleted Uranium. *J. Hazard. Mater.* **2019**, *364* (November 2017), 293–299. https://doi.org/10.1016/j.jhazmat.2018.08.018.

(7) Fan, M.; Thongsri, T.; Axe, L.; Tyson, T. A. Using a Probabilistic Approach in an Ecological Risk Assessment Simulation Tool: Test Case for Depleted Uranium (DU). *Chemosphere* **2005**, *60* (1), 111–125. https://doi.org/10.1016/j.chemosphere.2004.12.004.

(8) McClain, D. E.; Benson, K. A.; Dalton, T. K.; Ejnik, J.; Emond, C. A.; Hodge, S. J.; Kalinich, J. F.; Landauer, M. A.; Miller, A. C.; Pellmar, T. C.; Stewart, M. D.; Villa, V.; Xu, J. Biological Effects of Embedded Depleted Uranium (DU): Summary of Armed Forces Radiobiology Research Institute Research. *Sci. Total Environ.* **2001**, *274* (1–3), 115–118. https://doi.org/10.1016/S0048-9697(01)00734-3.

(9) Katz, S. The Chemistry and Toxicology of Depleted Uranium. *Toxics* **2014**, *2* (1), 50–78. https://doi.org/10.3390/toxics2010050.

(10) Handley-Sidhu, S.; Bryan, N. D.; Worsfold, P. J.; Vaughan, D. J.; Livens, F. R.; Keith-Roach, M. J. Corrosion and Transport of Depleted Uranium in Sand-Rich Environments. *Chemosphere* **2009**, *77* (10), 1434–1439. https://doi.org/10.1016/j.chemosphere.2009.08.053.

(11) Bacon, J. R.; Davidson, C. M. Is There a Future for Sequential Chemical Extraction? *Analyst* **2008**, *133* (1), 25–46. https://doi.org/10.1039/b711896a.

(12) Vandenhove, H.; Vanhoudt, N.; Duquène, L.; Antunes, K.; Wannijn, J. Comparison of Two Sequential Extraction Procedures for Uranium Fractionation in Contaminated Soils. *J. Environ. Radioact.* **2014**, *137*, 1–9. https://doi.org/10.1016/j.jenvrad.2014.05.024.

(13) Rout, S.; Kumar, A.; Ravi, P. M.; Tripathi, R. M. Understanding the Solid Phase Chemical Fractionation of Uranium in Soil and Effect of Ageing. *J. Hazard. Mater.* **2016**, *317*, 457–465. https://doi.org/10.1016/j.jhazmat.2016.05.082.

(14) Ebinger, M.H., Kennedy, P.L., Myers, O.B., Clements, W., Bestgen, H.T., Beckman, R. J. *Long-Term Fate of Depleted Uranium at Aberdeen and Yuma Proving Grounds, Phase II: Human Health and Ecological Risk Assessments.*; Los Alamos, NM, 1996.

(15) U.S. climate data https://www.usclimatedata.com/climate/yuma/arizona/united-states/usaz0275 (accessed Sep 10, 2019).

(16) Holmes, J. G.; Jensen, C. A.; Marean, H. W.; Neill, N. P.; Root, A. S.; McLendon, W. E.; Burgess, J. L.; Strahorn, A. T.; Sweet, A. T. *Soil Survey of the Yuma Area, Arizona-California*; U.S. Department of Agriculture, 1905.

(17) Arizona-Sonora Desert Museum. Desert Soils https://www.desertmuseum.org/books/nhsd_desert_soils.php (accessed Sep 10, 2019).

(18) McComb, J. Q.; Rogers, C.; Han, F. X.; Tchounwou, P. B. Rapid Screening of Heavy Metals and Trace Elements in Environmental Samples Using Portable X-Ray Fluorescence Spectrometer, A Comparative Study. *Water, Air, Soil Pollut.* **2014**, *225* (12), 2169. https://doi.org/10.1007/s11270-014-2169-5.

(19) Sparks, D. L. *Methods of Soil Analysis- Part 1. Physical and Mineralogical Methods*; 1986.

(20) Rhoades, J. D.; Manteghi, N. A.; Shouse, P. J.; Alves, W. J. Estimating Soil Salinity from Saturated Soil-Paste Electrical Conductivity. *Soil Sci. Soc. Am. J.* **1989**, *53* (2), 428–433. https://doi.org/10.2136/sssaj1989.03615995005300020019x.

(21) Sparks, D. L. *Methods of Soil Analysis, Part 3. Chemical Methods*; 1996.

(22) Bouyoucos, G. S. Hydrometer Method Improved for Making Particle Size Analysis of Soils. *Agron. J.* **1962**, *54*, 464–465.

(23) Klute, A. Methods of Soil Analysis: Part 1—Physical and Mineralogical Methods; 1986; Vol. 9, pp 901–926. https://doi.org/10.2136/sssabookser5.1.2ed.c36.

(24) Sposito, G.; Lund, L. J.; Chang, A. C. Trace Metal Chemistry in Arid-Zone Field Soils Amended with Sewage Sludge: I. Fractionation of Ni, Cu, Zn, Cd, and Pb in Solid Phases1. *Soil Sci. Soc. Am. J.* **1982**, *46* (2), 260. https://doi.org/10.2136/sssaj1982.03615995004600020009x.

(25) Han, F. X.; Kingery, W. L.; Hargreaves, J. E.; Walker, T. W. Effects of Land Uses on Solid-Phase Distribution of Micronutrients in Selected Vertisols of the Mississippi River Delta. *Geoderma* **2007**, *142* (1–2), 96–103. https://doi.org/10.1016/j.geoderma.2007.08.006.

(26) Tessier, a; Campbell, P. G. C.; Bisson, M. Sequential Extraction Procedure for the Speciation of Particulate Trace Metals. *Anal. Chem.* **1979**, *51* (7), 844–851. https://doi.org/10.1021/ac50043a017.

(27) Han, F. X.; Banin, A. Solid-Phase Manganese Fractionation Changes in Saturated Arid-Zone Soils: Pathways and Kinetics. *Soil Sci. Soc. Am. J.* **1996**, *60* (4), 1072–1080. https://doi.org/10.2136/sssaj1996.03615995006000040016x.

(28) Aigberua, A. O. Effects of Spatial, Temporal and PH Changes on Fractionated Heavy Metals in Sediments of the Middleton River, Bayelsa State, Nigeria. *MOJ Toxicol.* **2018**, *4* (6). https://doi.org/10.15406/mojt.2018.04.00140.

(29) Gile, L. H.; Peterson, F. F.; Grossman, R. B. Morphological and Genetic Sequences of Carbonate Accumulation in Desert Soils. *Soil Sci.* **1966**, *101* (5).

(30) Environmental Protection Agency (EPA). *Depleted Uranium: Technical Brief*; 2006; Vol. 12.

(31) (IAEA), I. A. E. A. Depleted Uranium https://www.iaea.org/topics/spent-fuel-management/depleted-uranium.

(32) Zhang, Q.; Larson, S. L.; Ballard, J. H.; Cheah, P.; Kazery, J. A.; Knotek-Smith, H. M.; Han, F. X. A Novel Laboratory Simulation System to Uncover the Mechanisms of Uranium Upward Transport in a Desert Landscape. *MethodsX* **2019**, *7* (November 2019), 100758. https://doi.org/10.1016/j.mex.2019.11.031.

(33) Shomar, B.; Amr, M.; Al-Saad, K.; Mohieldeen, Y. Natural and Depleted Uranium in the Topsoil of Qatar: Is It Something to Worry About? *Appl. Geochemistry* **2013**, *37*, 203–211. https://doi.org/10.1016/j.apgeochem.2013.08.001.

(34) Bradford, G. R.; Change, A. C.; Page, A. L.; Bakhtar, D.; Frampton, J. A.; Wright, H. *Background Concentrations of Trace and Major Elements in California Soils*; 1996.

(35) Sauve, S.; Hendershot, W.; Allen, H. E. Solid-Solution Partitioning of Metals in Contaminated Soils: Dependence on PH, Total Metal Burden, and Organic Matter. *Environ. Sci. Technol.* **2000**, 1125–1131.

(36) Al-Saad, K. A.; Amr, M. A.; Ismail, A.; Helal, A. I. Determination of Depleted Uranium in the Presence of Natural Uranium in Environmental Soil Samples by ICP-MS after Sequential Extraction. *J. Environ. Chem. Ecotoxicol.* **2010**, *2* (4), 60–66.

(37) Kaplan, D. I.; Serkiz, S. M. Quantification of Thorium and Uranium Sorption to Contaminated Sediments. *J. Radioanal. Nucl. Chem.* **2001**, *248* (3), 529–535. https://doi.org/10.1023/A:1010606325979.

(38) Johnson, W. H.; Buck, B. J.; Brogonia, H.; Brock, A. L. Variations in Depleted Uranium Sorption and Solubility with Depth in Arid Soils. *Soil Sediment Contam. An Int. J.* **2004**, *13* (6), 533–544. https://doi.org/10.1080/10588330490519428.

(39) Khodaverdiloo, H.; Han, F. X.; Taghlidabad, R. H.; Karimi, A.; Moradi, N.; Kazery, J. A. Potentially Toxic Element Contamination of Arid and Semi-Arid Soils and Its Phytoremediation. *Arid L. Res. Manag.* **2020**, *0* (0), 1–31. https://doi.org/10.1080/15324982.2020.1746707.

(40) Brand, U.; Veizer, J. Chemical Diagenesis of a Multicomponent Carbonate System - 1: Trace Elements. *J. Sediment. Petrol.* **1980**, *50* (4), 987–998. https://doi.org/10.1306/212F7DF6-2B24-11D7-8648000102C1865D.

(41) Heikkinen, P. M.; Räisänen, M. L. Trace Metal and As Solid-Phase Speciation in Sulphide Mine Tailings - Indicators of Spatial Distribution of Sulphide Oxidation in Active Tailings Impoundments. *Appl. Geochemistry* **2009**, *24* (7), 1224–1237. https://doi.org/10.1016/j.apgeochem.2009.03.007.

(42) Medina, V. F.; Wynter, M.; Larson, S. L.; Moser, R. D.; Nestler, C. C. *Corrosion and Migration of Zero-Valent Depleted Uranium Products in Soil*; 2018.

(43) Shaheen, S. M.; Alessi, D. S.; Tack, F. M. G.; Ok, Y. S.; Kim, K. H.; Gustafsson, J. P.; Sparks, D. L.; Rinklebe, J. Redox Chemistry of Vanadium in Soils and Sediments: Interactions with Colloidal Materials, Mobilization, Speciation, and Relevant Environmental Implications - A Review. *Adv. Colloid Interface Sci.* **2019**, *265*, 1–13. https://doi.org/10.1016/j.cis.2019.01.002.

(44) Calvert, S. E.; Pedersen, T. F. Geochemistry of Recent Oxic and Anoxic Marine Sediments: Implications for the Geological Record. *Mar. Geol.* **1993**, *113* (1–2), 67–88. https://doi.org/10.1016/0025-3227(93)90150-T.

(45) Khalid, R. A.; Patrick, W. H.; Gambrels, R. P.; Gambrel, R. P. Effect of Dissolved Oxygen on Chemical Transformations of Heavy Metals, Phosphorus, and Nitrogen in an Estuarine Sediment ". *Estuar. Coast. Mar. Sci.* **1978**, *6*, 21–35.

(46) Han, F. X.; Banin, A. Long-Term Transformations and Redistribution of Potentially Toxic Heavy Metals in Arid-Zone Soils Incubated: I. Under Saturated Conditions. *Water. Air. Soil Pollut.* **1997**, *95* (1–4), 399–423. https://doi.org/10.1007/BF02406176.

(47) Abesser, C.; Robinson, R.; Soulsby, C. Iron and Manganese Cycling in the Storm Runoff of a Scottish Upland Catchment. *J. Hydrol.* **2006**, *326* (1–4), 59–78. https://doi.org/10.1016/j.jhydrol.2005.10.034.

(48) Pett-Ridge, J. C.; Monastra, V. M.; Derry, L. A.; Chadwick, O. A. Importance of Atmospheric Inputs and Fe-Oxides in Controlling Soil Uranium Budgets and Behavior along a Hawaiian Chronosequence. *Chem. Geol.* **2007**, *244* (3–4), 691–707. https://doi.org/10.1016/j.chemgeo.2007.07.016.

(49) Ching-kuo Daniel Hsi; Langmuir, D. Adsorption of Uranyl onto Ferric Oxyhydroxides: Application of the Surface Complexation Site-Binding Model. *Geochim. Cosmochim. Acta* **1985**, *49* (9), 1931–1941. https://doi.org/10.1016/0016-7037(85)90088-2.

(50) Ainsworth, C. C.; Pilon, J. L.; Gassman, P. L.; Sluys, W. G. Van Der. Cobalt, Cadmium, and Lead Sorption to Hydrous Iron Oxide: Residence Time Effect. *Soil Sci. Soc. Am. J.* **1994**, *58*, 1615–1623.

(51) McLaren, R. G.; Backes, C. A.; Rate, A. W.; Swift, R. S. Cadmium and Cobalt Desorption Kinetics from Soil Clays: Effect of Sorption Period. *Soil Sci. Soc. Am. J.* **1998**, *62* (2), 332. https://doi.org/10.2136/sssaj1998.03615995006200020006x.

(52) Trivedi, P.; Axe, L. Modeling Cd and Zn Sorption to Hydrous Metal Oxides. *Environ. Sci. Technol.* **2000**, *34* (11), 2215–2223. https://doi.org/10.1021/es991110c.

(53) Bartlett, R. J.; James, B. R. System for Categorizing Soil Redox Status by Chemical Field Testing. *Geoderma* **1995**, *68* (3), 211–218. https://doi.org/10.1016/0016-7061(95)00034-L.

(54) Han, F. X.; Banin, A.; Kingery, W. L.; Triplett, G. B.; Zhou, L. X.; Zheng, S. J.; Ding, W. X. New Approach to Studies of Heavy Metal Redistribution in Soil. *Adv. Environ. Res.* **2003**, *8* (1), 113–120. https://doi.org/10.1016/S1093-0191(02)00142-9.

(55) Bednar, A. J.; Medina, V. F.; Ulmer-Scholle, D. S.; Frey, B. A.; Johnson, B. L.; Brostoff, W. N.; Larson, S. L. Effects of Organic Matter on the Distribution of Uranium in Soil and Plant Matrices. *Chemosphere* **2007**, *70* (2), 237–247. https://doi.org/10.1016/j.chemosphere.2007.06.032.

(56) Shacklette, H. T.; Boerngen, J. G. Element Concentrations in Soils and Other Surfical Materials of the Conterminous United States. *U.S. Geol. Surv. Prof. Pap. 1270* **1984**, 1–63.

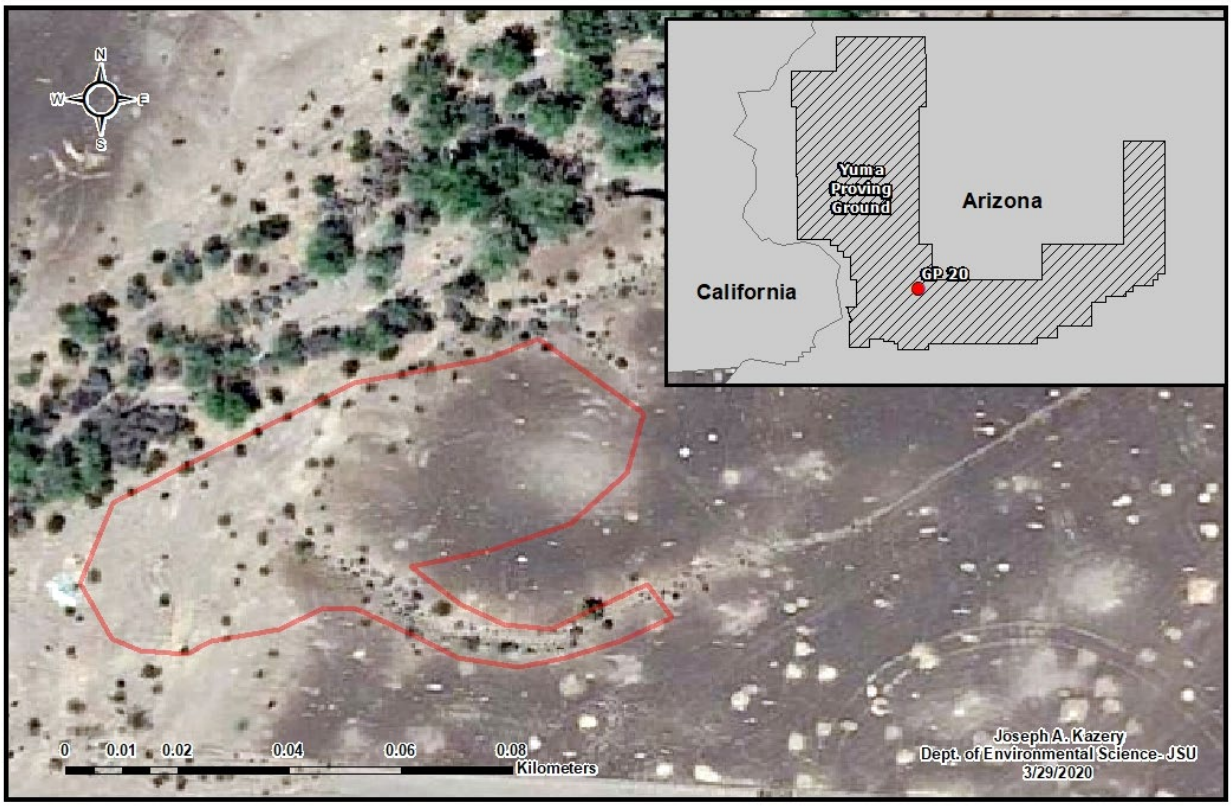

Figure 1. The landscape and the sampling area (outlined in red) at Gun Position 20 (GP 20) at Yuma Proving Ground in Arizona. Sampling area includes the flat open field and a lower elevated drainage trench.

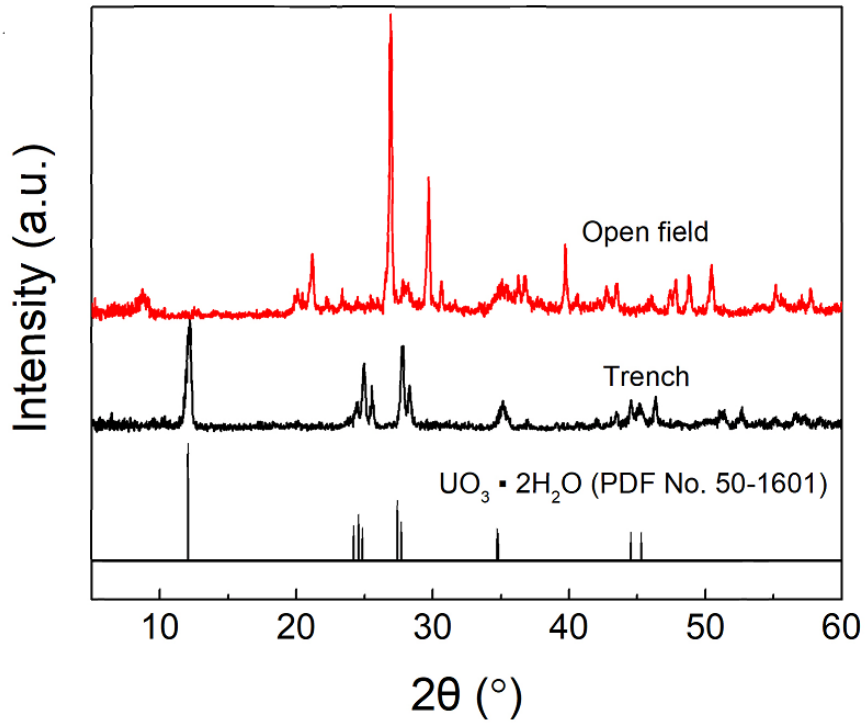

Figure 2. X-ray diffraction (XRD) analysis of corroded products of penetrators with the presence of schoepite found from open field and trench soil.

Figure 3. U distribution among solid phase components in soils from the open field and the trench areas at GP 20. Solid Phase Fractions: SOL, soluble; EXC, exchangeable; CARB, carbonate; ERO, easily reducible oxide; OM, organic matter; AmoFe, amorphous iron oxides; CryFe, crystalline iron oxides; and RES, residual fractions.

Table 1. Characterization and physicochemical properties of soils at GP20 in Yuma Proving Ground

	pH	EC (mS)EC (mS)	OM (%)	$CaCO_3$ (%)	Fe-oxides (mg/kg)	Mn-oxides (mg/kg)	Sand (%)	Silt (%)	Clay (%)
Mean	8.21	287.4	3.06	14.82	3627	123.7	51.83	32.08	16.09
Std dev	0.30	506.0	0.99	4.13	660.1	50.74	4.28	3.25	1.04
CV%	3.69	176.1	32.19	0.28	18.20	41.01	8.27	10.12	6.49
Max	8.87	1383	4.71	34.15	4751	258.1	56.64	34.56	17.00
Min	7.88	3.47	0.76	8.33	2592	46.89	48.44	28.41	14.95

Electric conductivity (EC); Organic matter (OM); Standard deviation (Std dev)

Table 2. Total content of uranium in soils collected from the open field area (n=20) and lower level trench (n=10) from GP 20 in Yuma Proving Ground.

Location	Mean (mg/kg)	Median (mg/kg)	Standard deviation	CV (%)	Minimum (mg/kg)	Maximum (mg/kg)
Open field	278.8	191.4	365.0	130.9	12.93	2282
Trench	124400	98000	80470	64.68	18960	287900
1996 study *	224700	42000	403800	179.7	0.00	1400000

* indicated trench data (n=22) collected from Ebinger et al. 1996.

Table 3. Statistical summary of the eight fractions of U at both of the sampling locations at GP 20

Location		SOL**	EXC**	CARB**	ERO**	OM*	AmoFe**	CryFe*	RES*
Open field	Mean (mg/kg)	0.00	5.699	47.32	0.0813	0.5621	139.4	2.222	25.56
	Std dev	0.00	11.66	136.5	0.6298	0.7345	157.9	6.152	55.13
	CV%	-	205	289	775	130	113	277	216
	Max (mg/kg)	0.00	73.78	1038	4.879	3.448	485.7	42.66	350.5
	Min (mg/kg)	0.00	0.00	0.5893	0.00	0.00	0.00	0.00	0.00
Trench	Mean (mg/kg)	421.1	2200	27860	94020	18.04	11750	131.4	65.74
	Std dev	462.8	1569	6069	98210	47.31	7195	301.1	66.05
	CV%	109.92	71.33	21.79	104.45	262.2	61.21	229.2	100.5
	Max (mg/kg)	1571	5479	38122	361700	165.0	26310	1321	206.7
	Min (mg/kg)	19.87	342.0	11466	0.00	0.00	1189	0.00	0.00

* and ** indicates that sample locations of the same fraction were significantly different at the probability level of 0.05 and 0.001, respectively. Water-soluble (SOL); Exchangeable (EXC); Carbonate (CARB); Easily-reducible oxides (ERO); Organic matter (OM); Amorphous iron-oxides (AmoFe); Crystalline iron-oxides (CryFe); Residual (RES); Standard deviation (Std dev).

Table 4. Total content of trace elements (mg/kg) in the open field and the trench soils.

Trace element	Open field	Trench
	mg/kg	
As*	7.60 ± 1.51	4.89 ± 1.57
Ba*	429.2 ± 157.2	220.0 ± 107.8
Co*	8.44 ± 0.97	4.31 ± 1.61
Cr*	27.38 ± 4.01	12.51 ± 5.25
Cu*	22.52 ± 2.94	13.64 ± 3.87
Hg	0.41 ± 0.60	0.45 ± 0.40
Mo	0.93 ± 0.13	0.85 ± 0.28
Nb*	0.31 ± 0.04	0.24 ± 0.04
Pb*	13.19 ± 2.30	7.38 ± 2.82
Pd*	3.80 ± 0.57	2.59 ± 0.45
V*	47.49 ± 6.14	20.20 ± 8.66
Zn*	65.74 ± 10.03	31.86 ± 12.04
Zr*	12.31 ± 1.65	10.16 2.72

*indicated the significant difference between U in the open field and in the trench at the p = 0.05 probability level. Data were presented as the means with standard deviation

Table 5. Mean concentrations of trace elements in solid phase components from the open field samples.

	V	Cr	Co	Cu	Zn	As	Zr	Nb	Mo	Pd	Ba	Hg	Pb	U
	mg/kg													
SOL	0.696	0.050	0.004	0.664	1.210	0.00	0.00	0.00	0.00	0.00	2.176	0.00	0.293	0.00
EXC	0.282	0.729	0.018	0.011	2.137	0.00	0.003	0.00	0.040	0.00	63.29	0.00	0.00	5.699
CARB	1.700	10.70	0.00	26.91	3.548	0.001	0.002	0.00	0.690	0.100	85.56	0.235	0.00	47.03
ERO	6.376	0.570	0.00	0.203	0.582	0.00	0.018	0.00	0.069	0.001	51.39	0.842	0.061	0.056
OM	10.02	2.371	1.105	1.091	5.420	0.195	0.00	0.00	0.00	0.082	63.51	17.16	3.556	0.149
AmoFe	7.014	4.483	0.203	9.180	10.31	2.934	7.531	0.607	0.116	0.086	36.58	0.00	1.422	139.4
CryFe	8.753	11.26	0.00	3.474	10.40	0.150	0.766	0.008	0.009	0.031	10.05	0.00	1.524	2.212
RES	21.38	16.25	1.163	7.867	26.73	0.239	4.479	0.007	0.017	0.079	70.31	0.019	2.336	25.56

Water-soluble (SOL); Exchangeable (EXC); Carbonate (CARB); Easily-reducible oxides (ERO); Organic matter (OM); Amorphous iron-oxides (AmoFe); Crystalline iron-oxides (CryFe); Residual (RES)